Journal of Asian Ceramic Societies 2 (2014) 248–252

Contents lists available at ScienceDirect

Journal of Asian Ceramic Societies

journal homepage: www.elsevier.com/locate/jascer

Influence of zinc incorporation on microstructure of hydroxyapatite to characterize the effect of pH and calcination temperatures

H. Esfahani, E. Salahi*, A. Tayebifard, M.R. Rahimipour, M. Keyanpour-Rad

Materials and Energy Research Center (MERC), P.O. Box 141554777, Tehran, Iran

ARTICLE INFO

Article history:
Received 27 February 2014
Received in revised form 6 May 2014
Accepted 7 May 2014
Available online 5 June 2014

Keywords:
Calcination
Hydroxyapatite
pH
Tri calcium phosphate
Zinc incorporation

ABSTRACT

This work was focused to study the existence of Zn^{2+} in structure, chemical composition as well as particle and crystallite size of hydroxyapatite (HAp) to characterize the effect of pH of the solution and calcination temperature. Non-stoichiometric HAp (nHAp) powders containing 4 at.% zinc fraction were synthesized via solution–precipitation method. In order to characterize the effect of pH (values: 9 and 10.5) and two calcination temperatures (550 and 1000 °C) on chemical composition, molecule internal bonds, particle and crystallite size of the synthesized powders, XRD, EDS, FTIR and SEM techniques were utilized. The results showed that zinc cations could be incorporated in the HAp atomic structure to form low crystalline single phase of nHAP. The pH adjustment to 10.5 caused the formation of powders with smaller particle and crystallite sizes. The results also indicated that calcination temperature up to 1000 °C caused decomposition of zinc doped nHAp to β-tri calcium phosphate and tri zinc calcium phosphate phases which are used to control the speed of biodegradation.

1. Introduction

Hydroxyapatite (HAp), the primary inorganic component of bone and teeth, has been widely used in many biomedical fields. HAp structure possesses great flexibility in accepting substitutions in its network and various ions can be replaced in the position of calcium or phosphate ions into the HAp structure [1,2]. Substitution groups may provoke typical changes in the lattice parameters, crystallinity, crystal symmetry, thermal stability, morphology, solubility, physical, chemical and biological characteristics [3]. The zinc cation (Zn) is one of the most important cations that can be incorporated in the Ca sites of HAp atomic structure. This cation has been found to be very osteoconductive and can stimulate osteogenesis [4–7].

In order to control speed of biodegradation, a biphasic calcium phosphate (BCP) bioceramic has been developed, containing both HAp and TCP phases. A biological HAp usually has a non-stoichiometric composition (nHAp) with general chemical formula as given in Eq. (1):

$$Ca_{10-x}(HPO_4)_x(PO_4)_{6-x}(OH)_{2-x} \quad (1)$$

β-TCP, which has almost the same chemical composition but a different crystalline structure from nHAp, is more soluble and allows the biological precipitation of apatites [3]. Recently the incorporation of Zn into the HAp structure has been the interesting subject of the researches [8–10]. Zn^{2+} is known to have an inhibitory effect on HAp formation and reduces the crystallinity of the HAp structure by promotion of the TCP formation [11]. The pH of the solution, the concentration of the mixing reagents, the preparation temperature as well as calcination temperature, all affect the chemical composition and particle size of the precipitated powders [12].

Calcium phosphate powders can be prepared by several synthetic routes which include hydrothermal, sol–gel, spray-pyrolysis processes and wet chemical methods [13,14]. In this work, zinc doped HAp nano powders were synthesized by using wet chemical precipitation method. The novelty of this work is to investigate how the zinc cations can change the atomic structure of HAp influence of pH of the solution and calcination temperature. Atomic structure and morphology of the products were studied by characterization techniques TG–DTA, EDS, X-ray diffraction, FTIR and SEM.

* Corresponding author at: Materials and Energy Research Center (MERC), POB: 31787 316, Meshkin dasht, Karaj, Iran. Tel.: +98 2636280040 9; fax: +98 2636280040 9.
E-mail addresses: h-esfahani@merc.ac.ir (H. Esfahani), e-salahi@merc.ac.ir (E. Salahi), a-tayebi@merc.ac.ir (A. Tayebifard), m-rahimi@merc.ac.ir (M.R. Rahimipour), m.kianpour984@yahoo.com (M. Keyanpour-Rad).
Peer review under responsibility of The Ceramic Society of Japan and the Korean Ceramic Society.

Production and hosting by Elsevier

2187-0764 © 2014 The Ceramic Society of Japan and the Korean Ceramic Society. Production and hosting by Elsevier B.V. All rights reserved.
http://dx.doi.org/10.1016/j.jascer.2014.05.001

2. Materials and methods

2.1. Preparation of Zn-incorporated HAp

Aqueous phosphorous and calcium salts solutions were separately prepared by dissolving 0.06 mol diammonium hydrogen phosphate ($(NH_4)_2HPO_4$, Merck, 99% pure, Art No. 1.01207.500) into 50 mL distilled water and by dissolving 0.1 mol hydrate calcium acetate ($Ca(CH_3COO)_2{\cdot}H_2O$, Merck, 99% pure, Art No. 1.09325.0500) into 50 mL distilled water. The latter solution was added dropwise to the former solution under vigorous stirring at 45 °C. The pH of the final solution was adjusted to 9 and 10.5 by addition of 0.1 M ammonia. The precipitated powders were dried at 80 °C for 10 h. In order to synthesize Zn incorporated HAp powders, similar to the above procedure, appropriate amount of dihydrate zinc acetate ($Zn(CH_3COO)_2{\cdot}2H_2O$, Merck, extra pure, Art No. 1.08802.0250) was added to hydrate calcium acetate solution. The (Ca + Zn)/P molar ratio was kept constant at 1.67 throughout the experiments. The amount of zinc was chosen to be 4 at.%, with regard to Zn/(Zn + Ca) fraction. Finally, the dried powders were calcined at 550 and 1000 °C to investigate the influence of zinc cation on chemical composition and the particle size of calcium phosphate resultant. The appropriate sample codes have been given in Table 1.

2.2. Characterizations

Thermogravimetric-Differential Thermal Analysis (STA 1460 Equipment) was used to discover suitable calcination temperatures. The phase analysis of synthesized powders was done by X-ray diffraction in the scanning range of $2\theta = 10–80°$ (Co-$k_\alpha 1 = 1.78901$ Å, Ni filtered); Philips PW2273 diffractometer. The phases developed during precipitation and also after calcination were compared using standard JCPDS files. FTIR analyses were performed using a Vector 33-Bruke spectrophotometer as the ASTM 1252 standard to investigate the structural changes of the material molecular bands. Morphology and chemical composition of the powders were evaluated, using scanning electron microscopy (VEGA-TESCAN) equipped to EDS analyzer. In order to determine the particle size, a drop of suspension of synthesized powders was deposited on glass slide and sputter-coated with 10 nm of gold and then the images were evaluated using an image analyzer. The crystallite size of the synthesized powders were determined from the X-ray line broadening using Sherrer's equation as follows [15]:

$$D = 0.9\lambda/\beta\cos\theta \quad (2)$$

where D is the crystallite size, λ is wavelength of the radiation, θ is the Bragg's angle and β is the full width at half maximum.

3. Results and discussion

3.1. Thermal behavior

TG–DTA analysis was carried out to determine suitable calcination temperatures. Fig. 1 shows the TG–DTA profiles of the samples. The weight loss below 150 °C and regarding endothermic peak in these temperatures is attributed to the desorption of water trapped in the surface of nHAP. Dehydration and condensation of

Table 1
Conditions of powder preparation and their codes.

Zn/(Ca + Zn)	pH 9		pH 10.5	
	25 °C	25 °C	550 °C	1000 °C
0	0ZH1	0ZH2	0ZH2-550	0ZH2-1000
4	4ZH1	4ZH2	4ZH2-550	4ZH2-1000

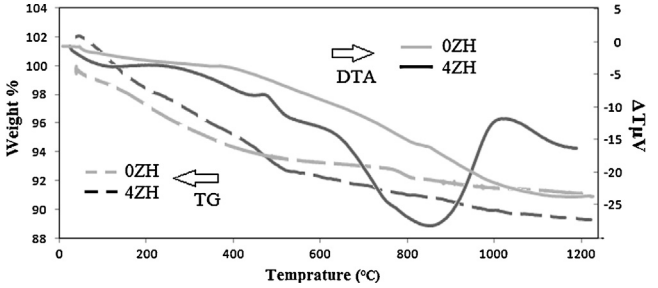

Fig. 1. TG–DTA profiles of the products. 0 at.% zinc fraction (grey lines) and 4 at.% zinc fraction (black lines).

HPO_4^{2-} group and also vaporization of the lattice water might occur in the range of 150–600 °C [16]. A weak peak was seen around 480 °C in DTA curve of 4ZH accompanied by loss of weight in its TGA graph indicating low range dehydration and condensation of HPO_4^{2-} group in 4ZH1 powders. Therefore, it can be expected that Zn^{2+} do not influence the atomic structure of HAp in temperatures below 600 °C. The significant peaks were not observed in the 0ZH1 sample in temperatures higher than 600 °C, indicating no formation or decomposition of new phase. But a wide endothermic peak was observed at 700–950 °C in the sample containing 4 at.% zinc fraction, indicating decomposition of the nHAp and formation of the tri calcium phosphate ($Ca_3(PO_4)_2$) and/or tri zinc phosphate ($Zn_3(PO_4)_2$). Broad mentioned peak reveals that decomposition takes place in wide temperature range. Therefore, to elucidate the effect of calcinations temperature on atomic structure of free zinc and zinc doped HAp 550 and 1000 °C temperature were candidate.

3.2. Chemical composition and phases

The EDS spectra of zinc free and zinc incorporated nHAp powders synthesized at pH 9 have been presented in Fig. 2. As it can be seen, their spectra have been overlapped except in the region of 0.8–1.2 keV which is shown by the circle and magnified in the right side of Fig. 2. The X-ray energy dispersed by Zn-L_α appears by doping of zinc into nHAp. Therefore, the presence of calcium, zinc

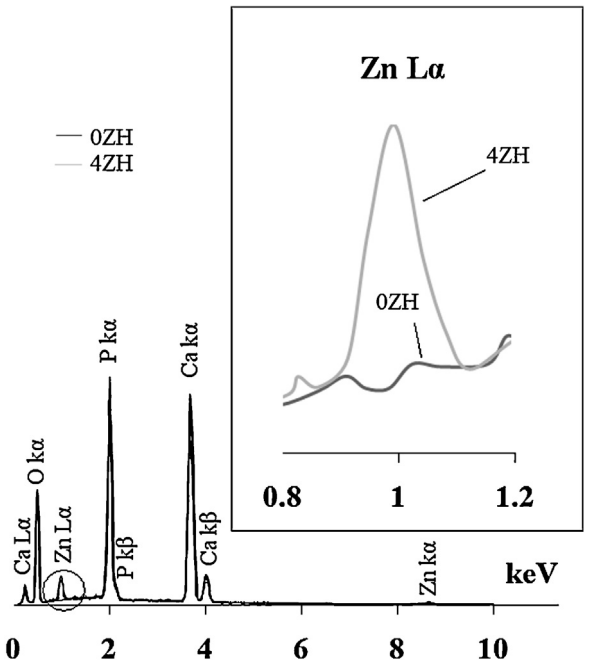

Fig. 2. The EDS spectra of entire and zinc incorporated nHAp.

and phosphorus was confirmed in both the samples. The estimated (Ca + Zn)/P molar ratio of the synthesized powders was 1.64 and 1.58 respectively for zinc free and incorporated samples. The EDS spectra and (Ca + Zn)/P molar ratios of both synthesized powders at pH 10.5 in different temperatures had similar consequences.

The X-ray pattern of zinc free and incorporated HAp powders synthesized in different pH values and also after calcination in different temperatures has been plotted in Fig. 3. The X-ray diffraction pattern of 0ZH1 and 4ZH1, as shown in Fig. 3(a) and (e), indicated that free zinc and incorporated calcium-phosphate powders have been formed in single crystalline nHAp phase. In comparison, incorporation of 4 at.% Zn^{2+} into HAp powders caused to decrease crystallinity of HAp powders which can be seen in Fig. 3(a) and (e). The XRD pattern of synthesized 0ZH2 and 4ZH2 showed that not only the new phase was not created by increasing the pH from 9 to 10.5 but also the crystallinity and scheme of the pattern of 0ZH powders were not changed by increasing the pH.

In a similar way, not only no new phases were formed by calcination of synthesized powders in 550 °C but also no significant changes occurred in crystallinity of both types of powders except a shifting peak with regard to (2 1 1) plane in the 4ZH sample. Because of the difference in ionic radius between Zn^{2+} (0.074 nm) and Ca^{2+} (0.099 nm) result in shift (2 1 1) plane to lower angle after the calcinations at 550 °C. These results have good agreement with prediction in TG–DTA analysis, where heat treatment at 550 °C would not cause change in the atomic structure of HAp drastically.

In contrast the XRD patterns of free zinc powders calcined at 1000 °C (Fig. 3(d)) were different from those obtained at 550 °C. The result showed that the high crystalline structure was achieved. A peak at $2\theta = 30.9°$ appeared in XRD pattern of sample 0ZH2 (Fig. 3(d)) with regard to β-tri calcium phosphate (β-TCP). It was found that the purity of HAp powders might be decreased by calcination at 1000 °C. Although high crystalline powder was synthesized in case contain 4 at.% zinc fraction too, but the XRD pattern was drastically different from the lines known as HAp structure. In comparison to 0ZH2 the β-TCP peak at $2\theta = 30.9°$ was intensified and new peaks with regard to another phase were accompanied in diffraction pattern of 4ZH2-1000. It can be considered that the incorporated Zn^{2+} cations were extracted from HAp structure to form tri zinc phosphate phase [$Zn_3(PO_4)_2$] by calcinations at 1000 °C.

3.3. Internal molecular bonds

FTIR spectra of free zinc and incorporated HAp synthesized in different pH values and temperatures have been shown in Fig. 4. Functional vibration bonds of PO_4^{3-}, OH^-, HPO_4^{2-} as well as CO_3^{2-} were identified at 560–600 cm^{-1} and 956–1031 cm^{-1}, 3576 cm^{-1}, 875 cm^{-1} and 1423–1565 cm^{-1} respectively in FTIR spectra of 0ZH1 and 4ZH1 powder samples (Fig. 4(a) and (e)). These bands are referred to nHAp with general chemical formula as given in Eq. (1). Carbon dioxide might be dissolved in solution as a common contaminant from the atmosphere during the precipitation process and then incorporated into the amorphous complex followed by penetration into low crystalline HAp. The dissolution of carbon dioxide from the atmosphere occurs by the following reaction (Eq. (3)) [17]:

$$CO_{2(g)} + 2OH_{(aq)}^{-} \rightarrow CO_{3(aq)}^{2-} + H_2O_{(l)} \quad (3)$$

By increasing the pH, no new functional group was appeared either disappeared in FTIR spectrum of both type powders (Fig. 4(b) and (f)) but mentioned groups were small shifted to new wave

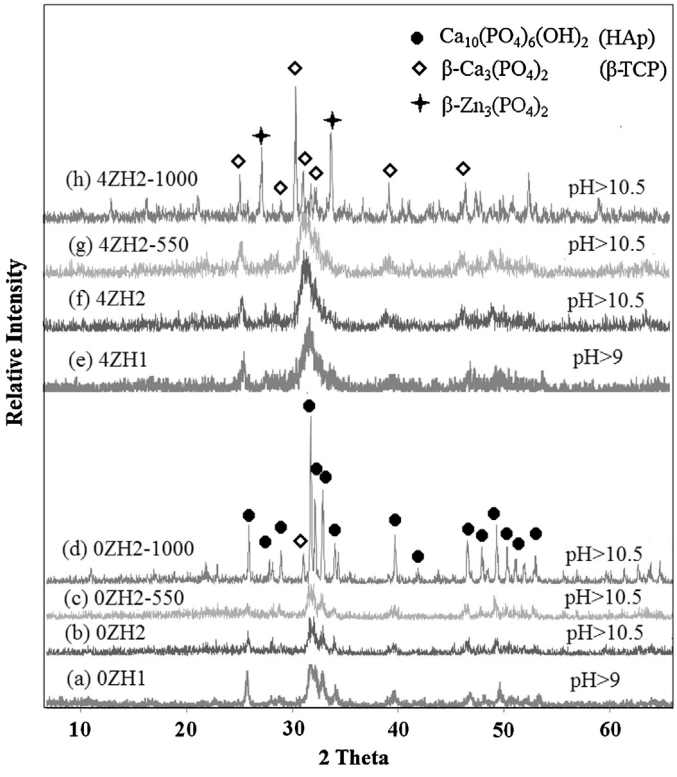

Fig. 3. The effect of pH values and temperature on X-ray diffraction pattern of (a) 0ZH1, (b) 0ZH2, (c) 0ZH2-550, (d) 0ZH2-1000, (e) 4ZH1, (f) 4ZH2, (g) 4ZH2-550 and (h) 4ZH2-1000.

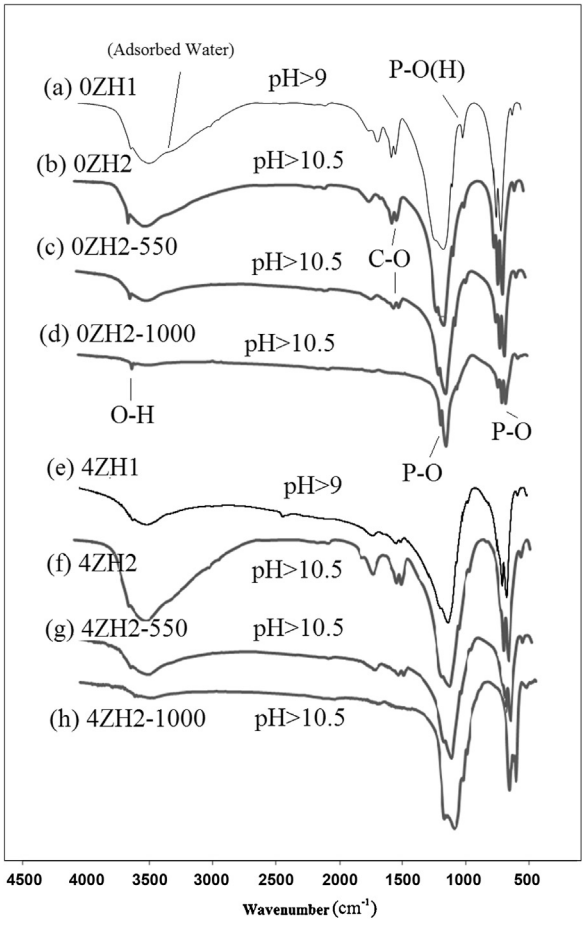

Fig. 4. The effect of pH values and temperature on FTIR spectrum of (a) 0ZH1, (b) 0ZH2, (c) 0ZH2-550, (d) 0ZH2-1000, (e) 4ZH1, (f) 4ZH2, (g) 4ZH2-550 and (h) 4ZH2-1000.

numbers and also in intensified. In comparison to the FTIR spectrum of 0ZH1 and 0ZH2, it can be found that P—O bonds in atomic structure of nHAp have been strengthened due to intensifying P—O band in FTIR spectra. Also P—(OH) band had appeared weaker in spectrum of 0ZH2 in comparison to the 0ZH1 sample. As can be seen, the FTIR spectrum of powders containing 4 at.% Zn was not drastically different from the undoped nHAp, except for transmitted bands of P—O(H) at 875 cm^{-1} and O—H at 3576 cm^{-1} which have been decreased by an influence of pH adjustment. The feature of P—O band was also changed by doping the zinc contaminate that it can be interpreted to decrease the crystallinity in agreement by the XRD results. Although formation of calcium vacancies via preparation of zinc doped HAp prevents to incorporation of CO_3^{2-} into HAp atomic structure due to opposition of electrostatic charges, but increasing of pH causes to increase the incorporation of CO_3^{2-} in to crystalline of HAp in accordance to Eq. (3). Therefore, no significant changes occurred in the carbonate band in FTIR spectrum of both synthesized powders via pH adjustment.

The calcination at 500 °C caused decrease of wide O—H band with regard to adsorbed H_2O at 3500 cm^{-1}. Hence adjacent O—H band attributed to functional group in nHAp structure distinctly appeared. Also calcination tend to appear weak CO_3^{2-} band. The calcination at 1000 °C caused discharge of adsorbed water from samples. Calcination affected the incorporation of carbonate in atomic structure of nHAp while C—O bands disappeared in FTIR spectra of free zinc and doped in nHAP (Fig. 4(d) and (h)). The FTIR spectrum of sample 0ZH indicated that it was included in the main functional group such as PO_4^{3-} and OH^- after calcination at 1000 °C. In addition, a shoulder has been appeared next to P—O band regarding to crystallinity changes of nHAp. Therefore, it can be found that HAp and TCP phases were formed in recent case which had good agreement with the XRD data. In contrast, FTIR of 4ZH2-1000 sample was included only in PO_4^{3-} group. Therefore, it can be elucidated that calcium and zinc atoms have bonded to PO_4^{3-} ionic group as TCP or tri-zinc phosphate. The XRD pattern of this sample, as shown in Fig. 4(h), indicated that calcium phosphate and zinc phosphate were dominant phases.

3.4. Crystallite and particle size

The measured average particle and crystallite size of doped and undoped zinc into nHAp synthesized in different pH and temperatures have been illustrated in Fig. 5. According to the results pH rising and zinc doping tend to form smaller particle size in both compositions. The SEM study confirmed nano crystalline nature of the materials which was calculated by Scherrer method. The results indicated that the size of the crystallites increased in coincidence to particles by increasing the calcinations temperature. The crystallite and particles grew by increasing the temperature to 550 °C. The zinc doped nHAp particles had 52% particle growth while 0ZH particles had 23%. Since XRD and FTIR results obtained at 550 °C showed unchangeable composition and phase in both powders, expansion of crystallite depended on lattice network expansion and subsequently the particle size was increased. In addition, in higher calcination temperature (1000 °C) resulted to form coarser particles with larger crystallite size. The average particle size was 120 ± 14 and 145 ± 18 nm, respectively, for free zinc and zinc incorporated powders. In contrast, 0ZH particles with 350 growing percentage had more expansion than those 4ZH particles with 280% particle growth. It was found that heat treatment only spent to expansion the crystal of HAp, but in case containing Zn^{2+} caused to decompose to new composition with lower particle size than origin HAp. Hence crystallite size of 4ZH powders was achieved lower than those in 0ZH powders corresponding to product new particles with mentioned composition.

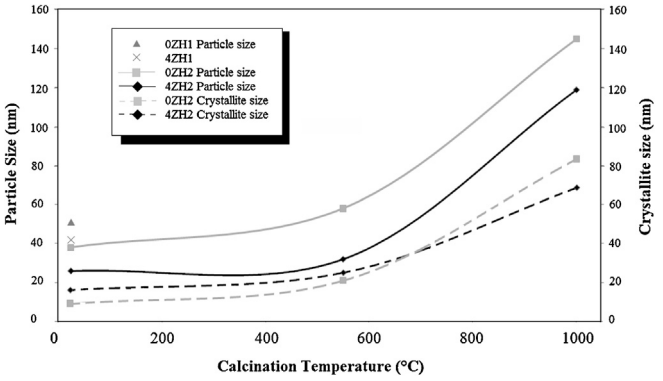

Fig. 5. Average particle size and crystallite size of the synthesized powders at different condition versus calcination temperatures.

The SEM images of particles calcined at 1000 °C typically are shown in Fig. 6(a) and (b). The representative particles of free zinc

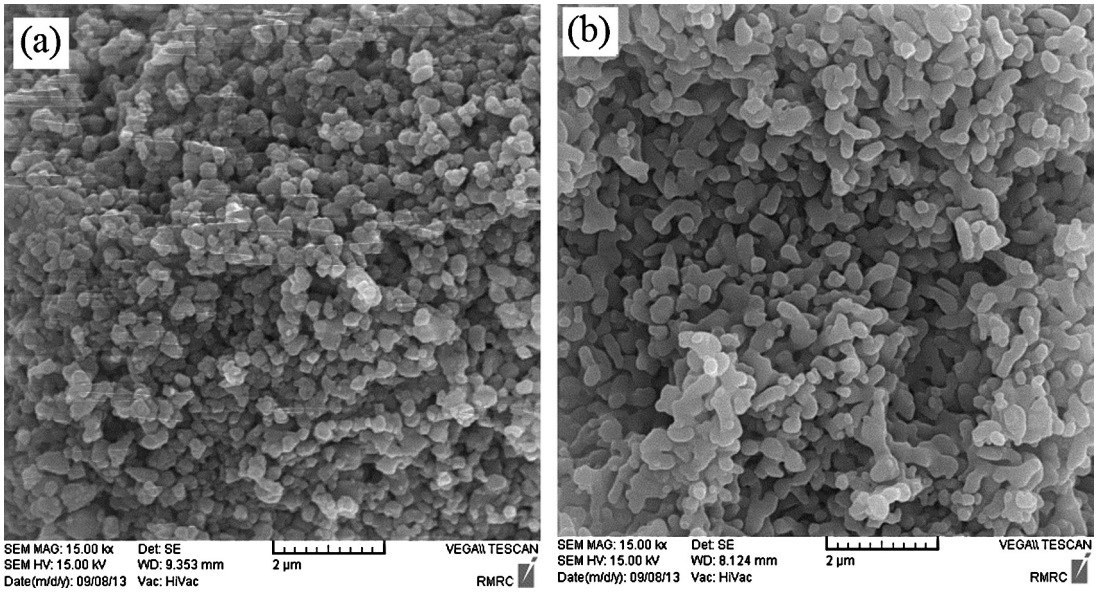

Fig. 6. SEM images of synthesized powders with different composition. (a) Entire and (b) Zn incorporated nHAp. pH 10.5 and $T = 1000$ °C.

and zinc doped nHAp are more uniform in size and irregular shape in both cases.

4. Conclusion

The effect of pH and calcination on structure, chemical composition and also particle size of zinc incorporated HAp was investigated. The XRD and FTIR results of both zinc free and zinc incorporated powders indicated that crystalline single phase of HAp has been precipitated. The EDS analysis showed that nHAp was formed. The pH adjustment and calcination at 550 °C did not influence the phase formation but calcination of zinc free powder at 1000 °C caused the formation of crystallized HAp with a few amount of β-TCP. Incorporated zinc cations decomposed nHAP to TCP and TZP. The pH adjustment to 10.5 caused to precipitate smaller particle size either smaller crystallite size. The SEM study indicated that zinc doped nHAp powders were more effected by calcination than devoid of zinc powders. The SEM images also showed uniform size, and irregular shaped particles were formed in both cases. According to the results, it can be concluded that calcination at 1000 °C caused the formation of biphasic calcium and zinc phosphate which is a good choice for using it in control speed biodegradation.

References

[1] P. Moghimian, A. Najafi, A. Afshar and J. Javadpour, Adv. Powder Technol., 23, (6) 744–751 (2012).
[2] K. Shitara, H. Murata, K. Watanabe, C. Kojima, Y. Sumida, A. Nakamura, A. Nakahira, I. Tanaka and K. Matsunaga, J. Asian Ceram. Soc., 2, (1) 64–67 (2014).
[3] S.C. Cox, P. Jamshidi, L.M. Grover and K.K. Mallick, Mater. Sci. Eng. C, 35, 106–114 (2014).
[4] D. Xie, I.D. Chung, G. Wang, D. Feng and J. Mays, Eur. Polym. J., 40, 1723–1731 (2004).
[5] K. Ishikaw, Y. Miyamoto, T. Yuasa, A. Ito, M. Nagayama and K. Suzuki, Biomaterials, 23, (2) 423–428 (2002).
[6] P. Bhattacharjee, H. Begam, A. Chanda and S.K. Nandi, J. Asian Ceram. Soc., 2, (1) 64–67 (2014).
[7] R.M.B. Faria, D.V. Cesar and V.M.M. Salim, Catal. Today, 133, 168–173 (2008).
[8] I. Uysal, F. Severcan and Z. Evis, Ceram. Int., 39, (7) 7727–7733 (2013).
[9] E. Fujii, M. Ohkubo, K. Tsuru, S. Hayakawa, A. Osaka, K. Kawabata, C. Bonhomme and F. Babonneau, Acta Biomater., 2, (1) 69–74 (2006).
[10] K. Kawabata, T. Yamamoto and A. Kitada, J. Phys. B, 406, 890–894 (2011).
[11] A. Rezakhani and M.M. Kashani Motlagh, Int. J. Phys. Sci., 7, (20) 2768–2774 (2012).
[12] S.V. Dorozhkin, Acta Biomater., 6, 4457–4475 (2010).
[13] A. Gozalian, A. Behnamghadera, M. Daliri and A. Moshkforoush, Sci. Iran. F, 18, (6) 1614–1622 (2011).
[14] I. Cacciotti and A. Bianco, Ceram. Int., 37, (1) 127–137 (2011).
[15] B.B. Cullity and B. Dennis, Directions of Diffracted Beams, Elements of X-ray Diffraction, 3rd ed., Addison-Wesley, Massachusetts (2001).
[16] F. Miyaji, Y. Kono and Y. Suyama, Mater. Res. Bull., 40, 209–220 (2005).
[17] S. Kongsri, K. Janpradit, K. Buapa, S. Techawongstien and S. Chant, Chem. Eng. J., 215–216, 522–532 (2013).